SLAC–PUB–5013
June 1989
T

TESTS OF QUANTUM CHROMODYNAMICS IN EXCLUSIVE AND INCLUSIVE ELECTROPRODUCTION*

STANLEY J. BRODSKY

Stanford Linear Accelerator Center, Stanford University, Stanford, California 94309, USA

1. INTRODUCTION

A scanning transmission electron microscope[1] provides an image of a specimen by combining information from both the elastically and inelastically scattered electrons that emerge after passing through the target. A high energy electroproduction experiment which measures both exclusive and inclusive reactions is a close analog of an electron microscope, providing images of the nucleon and nucleus at a resolution scale $\lambda \sim 1/Q$ where $Q^2 = -(p_e - p'_e)^2$ is the momentum transfer squared. Electroproduction on an internal gas jet target in a circulating electron ring has the potential to provide even more information: because of its high luminosity, good duty factor, and large angular acceptance, one can examine detailed properties of the hadronic final state in coincidence with the scattered electron. Moreover, if the proton or nuclear target is polarized, one can study detailed correlations of the target spin with properties of the produced hadrons. Using nuclear targets, one can systematically study the effects of varying the nuclear environment on each exclusive and semi-inclusive final state.

The proposed *PEGASYS* experiment at SLAC will utilize an internal gas jet target in the circulating *PEP* beam at $E_e \simeq 15\ GeV$ and thus can probe the structure of the nucleon or nucleus at center of mass energies $W^2 = (q+p)^2 \leq 30\ GeV^2$ and momentum transfers $Q^2 \leq 15\ GeV/c^2$. At such resolution, $\lambda < 10^{-14}$ cm, the quark and gluon structure of matter becomes apparent; one can test not only the predictions and dynamical mechanisms of quantum chromodynamics, but one also probe the structure of the hadron and nuclear wavefunctions in terms of their fundamental degrees of freedom. The large acceptance of the *PEGASYS* apparatus and the ability to do coincidence measurements will allow the study of the final state, channel by channel, as a function of the virtual photon mass below and above the Bjorken scaling regime. The *PEGASYS* kinematic range interpolates between the lower energy CEBAF domain where quark degrees of freedom begin to become manifest, and the much higher energies of HERA, which is far into the perturbative QCD regime of logarithmic evolution and multi-jet structure.

QCD itself is a theory of moderate energy scale. The parameter $\Lambda_{\overline{MS}}$ is conventionally used to set the scale where the running coupling constant $\alpha_s(Q^2)$ becomes large and thus perturbative expansions break down. Recent determinations using Υ decay and the multijet distributions[2] in e^+e^- annihilation suggest that $\Lambda_{\overline{MS}}$ is below 200 MeV and is perhaps as small as 100 MeV. In order to determine the absolute value of $\Lambda_{\overline{MS}}$ one must know the correct argument Q^* of the running coupling constant appropriate to the measurement. The above determinations of $\Lambda_{\overline{MS}}$ use the method of Ref. 3 in which this scale is determined "automatically" by requiring that light fermion pairs contributions are summed by the running coupling constant, just as is done in Abelian QED.

The effective masses of the u, d, and s quarks and their characteristic transverse momentum within hadrons are also of order of a few hundred MeV or less. Thus electron scattering at momentum transfers of $Q^2 \sim 5$ to 10 GeV^2, corresponding to resolution $\lambda \sim 0.1\ fm$, is clearly sufficient to resolve the structure of the nucleon and nucleus in terms of individual quark and gluon degrees of freedom. This is confirmed by the fact that the Bjorken scaling of the inelastic electron scattering cross section, which reflects the point-like scale-invariant behavior of the electron-quark interaction, is already apparent at momentum transfers Q^2 as low as 1 GeV/c^2.

The EMC and SLAC data on polarized structure functions imply significant correlations between the spin of the target proton with the spin of the gluons and strange quarks. Thus there should be significant correlations between the target spin and spin observables in the electroproduction final state, both in the current and target fragmentation region. It thus would be interesting to measure the spin of specific hadrons which are helicity self-analyzing through their decay products such as the ρ and the Λ.

It is useful to keep in mind the following simple model for the helicity parallel and helicity anti-parallel gluon distributions in the nucleon: $G^+_{g/N}(x) = \frac{3}{2}(1-x)^4/x$ and $G^-_{g/N}(x) = \frac{3}{2}(1-x)^6/x$, respectively. This model is consistent with the measured momentum, correct crossing behavior, dimensional counting rules at $x \to 1$, and Regge behavior at small x. It implies that more of the nucleon spin is carried by gluons rather than quarks.[4]

The analyses of the EMC and SLAC spin dependent structure functions as well as elastic neutrino-proton scattering imply substantial strange and anti-strange quarks in the proton, highly spin correlated with the proton spin. The usual description of the

* Work supported by the Department of Energy, contract DE–AC03–76SF00515.

Presented at the Topical Conference on Electronuclear Physics
with Internal Targets, Stanford, January 9–12, 1989

strange sea assumes that $s\bar{s}$ is strictly due to the simple gluon splitting process. The spin correlation of the strange quarks then requires a very large gluon spin correlation, much stronger than the simple model given above. Alternatively the strange sea may be "intrinsic" to the bound state equation of motion of the nucleon and thus the strong strange spin correlation may be a non-perturbative phenomena. One expects contributions at order $1/m_s^2$ to the strange sea from cuts of strange loops quark loops in the wavefunction with 2, 3, and 4 gluons connecting to the other quark and gluon constituents of the nucleon. Alternatively, one can regard the strange sea as a manifestation of intermediate $K - \Lambda$ and other virtual meson-baryon pair states in the fluctuations of the proton ground state.

Experiments which examine the entire final state in electroproduction can discriminate between these extrinsic and intrinsic components to the strange sea. For example, consider events in which a strange hadron is observed at large z in the fragmentation region of the recoil jet, signifying the production and tagging of a strange quark. In the case of intrinsic strangeness, the associated $\bar{s}$ will be in the target fragmentation region. In the case that the strange quark is created extrinsically via $\gamma^* g \to s\bar{s}$, both the tagged s quark and the $\bar{s}$ hadrons will be found predominantly in the current fragmentation region.

The use of nuclear targets in electroproduction allows one to probe effects specific to the physics of the nucleus itself such as the short-distance structure of the deuteron, high momentum nucleon-nucleon components, and coherent effects such as shadowing, anti-shadowing, and $x > 1$ behavior. However, perhaps the most interesting aspect for high energy physics is the use of the nucleus to modify the environment in which quark hadronization and particle formation occurs. The *PEGASYS* kinematic domain seems ideal to test the onset of "formation zone phenomena", "target length conditions", etc. It can also test an important principle controlling quark hadronization into exclusive channels inside nuclei: "color transparency".[5] Suppose that a hadronic state has a small transverse size $b_\perp$. Because of the cancellation of gluonic interactions with wavelength smaller than $b_\perp$, such a small color-singlet hadronic state will propagate through the nucleus with a small cross section for interacting in either elastically or inelastically. In particular, the recoil proton in large momentum transfer electron-proton scattering is produced initially as a small color singlet three-quark state of transverse size $b_\perp \sim 1/Q$. If the electron-proton scattering occurs inside a nuclear target (quasi-elastic scattering) then the recoil nucleon can propagate through the nuclear volume without significant final-state interactions. This perturbative QCD prediction is in striking contrast to standard treatments of quasi-elastic scattering which predict significant final state scattering and absorption in the nucleus due to large elastic and inelastic nucleon-nucleon cross sections. The theoretical calculations of the color transparency effect must also take into account the expansion of the state as it evolves to a normal proton of normal transverse size while it traverses the nucleus. We discuss color transparency further in Section 6.

2. Overview of Electroproduction Phenomenology

The central focus of inelastic electroproduction is the electron-quark interaction, which at large momentum transfer can be calculated as an incoherent sum of individual quark contributions. The deep inelastic electron-proton cross section is thus given by the convolution of the electron-quark cross section times the structure functions, or equivalently the probability distributions $G_{q/p}(x, Q^2)$. In the "infinite momentum frame" where the proton has large momentum P^μ and the virtual photon momentum is in the transverse direction, $G_{q/p}(x, Q^2)$ is the probability of finding a quark q with momentum fraction $x = Q^2/2p \cdot q$ in the proton. However in the rest frame of the target, many different physical processes occur: the photon can scatter out a quark as in the atomic physics photoelectric effect, it can hit a quark which created from a vacuum fluctuation near the proton, or the photon can first make a $q\bar{q}$ pair, either of which can interact in the target. Thus the electron interacts with quarks which are both *intrinsic* to the proton's structure itself, or quarks which are *extrinsic; i.e.* created in the electron-proton collision itself. Much of the phenomena at small values of x such as Regge behavior, sea distributions associated with photon-gluon fusion processes, and shadowing in nuclear structure functions can be identified with the extrinsic interactions, rather than processes directly connected with the proton's intrinsic structure.

There is an amusing, though *gedanken* way to (in principle) separate the extrinsic and intrinsic contributions to the proton's structure functions. For example, suppose that one wishes to isolate the intrinsic contribution $G^I_{d/p}(x, Q)$ to the d-quark distribution in the proton. Let us imagine that there exists another set of quarks $\{q_o\} = u_o, d_o, s_o, c_o, ...$ identical in all respects to the usual set of quarks but carrying zero electromagnetic and weak charges. The experimentalist could then measure the difference in scattering of electrons on protons versus electrons scattering on a new baryon with valence quarks $|uud_o>$. This is analogous to an "empty target" subtraction. Contributions from $q\bar{q}$ pair production in the gluonic field of the target (photon-gluon fusion) essentially cancel, so that one can then identify the difference in scattering with the intrinsic d-quark distribution of the nucleon. Because of the Pauli principle, $d\bar{d}$ production on the proton where the d is produced in

the same quantum state as the d in the nucleon is absent, but the corresponding contribution is allowed in the case of the $|uud_o>$ target. Because of this extra subtraction, the contributions associated with Reggeon exchange also cancel in the difference, and thus the intrinsic structure function $G^I(x,Q)$ vanishes at $x \to 0$. The intrinsic contribution gives finite expectation values for the light-cone kinetic energy operator, "sigma" terms, and the $J = 0$ fixed poles associated with $< 1/x >$.[6]

Although there have been extensive measurements of the deep inelastic structure functions, some aspects remain to be verified, and will require data over a large range of Q^2. For example, how much of the scale violation is due to power-law (higher twist) contributions[7] versus logarithmic PQCD evolution? Does the Bjorken-scaling non-isosinglet structure function $F_2(x,Q)$ behave as $Cx^{1-\alpha_\rho}$ as $x \to 0$ as dictated by Regge exchange and duality or is this a manifestation of higher twist contributions to the virtual photo-absorption cross section which falls as $1/Q^2$? Are the non-additive shadowing and anti-shadowing nuclear effects really leading twist or are they Q^2 dependent?

Electron-proton scattering also involves additional processes such as photoproduction, Compton processes, QED radiative corrections, etc. Electroproduction reactions in which large transverse momentum photons appear are particularly interesting. In the exclusive process $e^\pm p \to e^\pm \gamma p$ one can isolate the virtual Compton cross section as well as the real part of the Compton amplitude. In the inclusive reaction $e^\pm p \to e^\pm \gamma X$ one can determine reactions and sum rules proportional to the quark charge cubed.

It is thus interesting to consider inclusive electron-proton collisions from a general point of view. As long as there is at least one particle detected at large transverse momentum, whether it is a scattered electron, or a produced hard photon, or a hadron at large P_T, one can use the factorization formula[8]

$$\frac{d\sigma(AB \to CX)}{d^3p_c/E_c} \cong \sum_{ab,cd} \int_0^1 dx_a \int_0^1 dx_b \int_0^1 \frac{dx_c}{x_c^2}$$

$$\times G_{a/A}(x_a,Q) G_{b/B}(x_b,Q) \tilde{G}_{C/c}(x_c,Q)$$

$$\times \delta(s' + t' + u') \frac{s'}{\pi} \frac{d\sigma}{dt'}(ab \to cd)$$

which has general validity in gauge theory. The systems A, B, C can be leptons, photons, hadrons, or nuclei. The primary subprocess in electroproduction is $eq \to eq$. The electron structure function $G_{e/e}(x,Q)$ automatically provides the (leading logarithmic) QED radiative corrections. The spectrum of the electron beam plays the role of the non-perturbative or initial structure function. (See Fig. 1(b).) The subprocess $\gamma^* q \to gq$ corresponds to photon-induced two-jet production. (See Fig. 1(a).) This subprocess dominates reactions in which the large transverse momentum trigger is a hadron rather than the scattered lepton. Thus one sees that conventional deep inelastic $eq \to eq$ scattering subprocess is just one of the several modes of electroproduction.

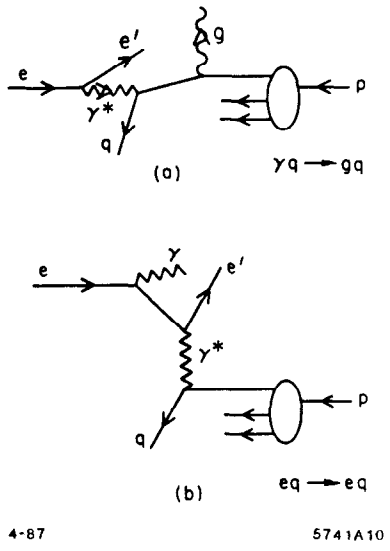

Figure 1. Application of gauge theory factorization to electroproduction. (a) The $\gamma q \to gq$ subprocess produces hadron jets at high p_T. (b) The $eq \to eq$ produces one quark jet and one recoil electron jet at high p_T. The QED radiative corrections are incorporated into the electron and photon QED structure functions.

The dominant contribution to the meson semi-inclusive cross section is predicted by QCD factorization to be due to jet fragmentation from the recoil quark and spectator diquark jets.

Higher Twist Effects

When the momentum transfer is in the intermediate range $1 \lesssim Q^2 \lesssim 10$ GeV^2, several other contributions for meson production are expected to become important in $eN \to e'MX$. These include:

1. Higher twist contributions to jet fragmentation:
$$\frac{dN_\pi}{dz} = D_{\pi/q}(z,Q^2) \cong A(1-z)^2 + \frac{C}{Q^2} \quad (z \to 1).$$
The scaling term reflects the behavior of the pion fragmentation function at large fractional momentum ($z \to 1$) as predicted by perturbative QCD (one-gluon exchange). (See

Fig. 2(a).) The C/Q^2 term[9] is computed from the same perturbative diagrams. For large z where this term dominates, we predict that the deep inelastic cross section will be dominantly longitudinal rather than transverse $R = \sigma_L/\sigma_T > 1$.

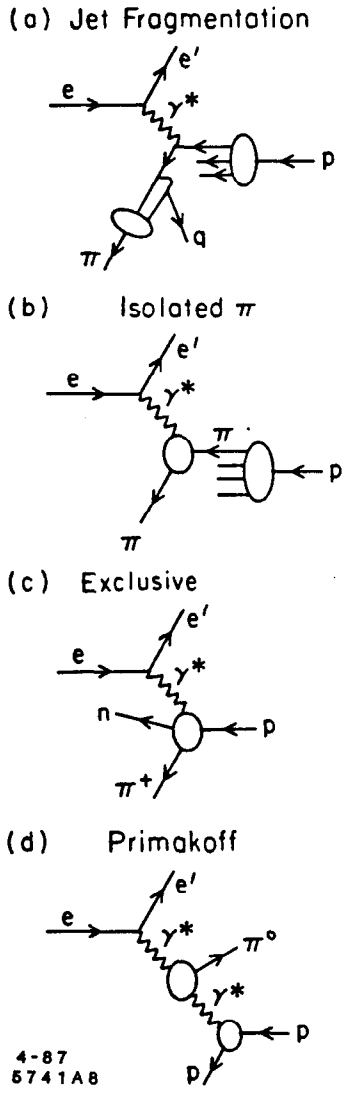

Figure 2. QCD contributions to pion electroproduction. (a) Jet fragmentation, including leading and $1/Q^2$ higher twist contributions. (b) Isolated pion contributions at order $1/Q^4$. (c) Exclusive production. (d) Primakoff contribution.

2. "Direct" meson production. Isolated pions may also be created by elastic scattering off of an effective pion current: (See Fig. 2(b).)

$$\frac{d\sigma}{dQ^2 dx_\pi} = G_{\pi/p}(x_\pi) \left.\frac{d\sigma}{dQ^2}\right|_{e\pi\to e\pi}$$

$$\left.\frac{d\sigma}{dy dQ^2}\right|_{e\pi\to e\pi} = \frac{4\pi\alpha^2}{(Q^2)^2} |F_\pi(Q^2)|^2 (1-y) .$$

Here $y = q\cdot p/p_e \cdot p$. In the case of a nuclear target, one can test for non-additivity of virtual pions due to nuclear effects, as predicted in models[10] for the EMC effect[11] at small x_{Bj}. Jaffe and Hoodbhoy[12] have shown that the existence of quark exchange diagrams involving quarks of different nucleons in the nucleus invalidates general applicability of the simplest convolution formulae conventionally used in such analyses. The $G_{\pi/p}(x,Q)$ structure function is predicted to behave roughly as $(1-x)^5$ at large x, as predicted from spectator quark counting rules.[14,8] Applications of these rules to other off-shell nucleon processes are discussed in Refs. 15 and 13.

3. Exclusive Channels. (See Fig. 2(c).) The mesons can of course be produced in exclusive channels; e.g. $\gamma^* p \to \pi^+ n$, $\gamma^* p \to \rho^0 p$. Pion electroproduction extrapolated to $t = m_\pi^2$ provides the basic knowledge of the pion form factor at spacelike Q^2. With the advent of the perturbative QCD analyses of large momentum transfer exclusive reactions, predictions can be given over the whole range of large t and Q^2. Exclusive processes are discussed in more detail in Section 7. We also discuss some special features of ρ^0 electroproduction in Section 9.

4. Another meson production channel is the Primakoff reaction $\gamma^*\gamma \to \pi^0$, etc., which dominates over other events at very low target recoil momentum. (See Fig. 2(d).) Such measurements would allow the determination of the $\gamma \to \pi^0$ transition form factor. This quantity, combined with the QCD analysis of the pion form factor leads to a method to determine the QCD running coupling constant $\alpha_s(Q^2)$ solely from exclusive measurements.[16]

3. Hadronization of the Quark and Spectator Systems

At its most basic level, Bjorken scaling of deep inelastic structure functions implies the production of a single quark jet, recoiling against the scattered lepton. The spectator system–the remnant of the target remaining after the scattered quark is removed–is a color-$\bar{3}$ system. The struck quark is sensitive to the magnitude of the momentum transfer Q and logarithmically evolves by radiated gluons with relative transverse momentum controlled by Q^2 and

the available phase-space. According to QCD factorization, the recoiling quark jet, together with the gluonic radiation produced in the scattering process, produces hadrons in a universal way, independent of the target or particular hard scattering reaction. This jet should be identical to the light quark jets produced in e^+e^- annihilation. In contrast, the hadronization of the spectator system depends in detail on the target properties. Unlike the quark jet, the leading particles of the target spectator system do not evolve and thus should not depend on the momentum transfer Q^2 [at fixed $W^2 = (q+p)^2$]. At present we do not have a basic understanding of the physics of hadronization, although phenomenological approaches, such as the Lund string model, have been successful in parameterizing many features of the data.

4. Hadronization in Nuclei

The study of electroproduction in nuclear targets gives the experimentalist the extraordinary ability to modify the environment in which hadronization occurs. The essential question is how the nucleus changes or influences the mechanism in which the struck quark and the spectator system of the target nucleon form final state hadrons.

There are several general properties of the effect of the nuclear environment which follow from the structure of gauge theory. The first effect is the "formation zone" which reflects the principle that a quark or hadron can change state only after a finite intrinsic time in its rest system. This implies that the scattered quark in electroproduction cannot suffer an inelastic reaction with mass squared change ΔM^2 while propagating a distance L if its laboratory energy is greater than $\Delta M^2 L$. However the outgoing quark can still scatter elastically as it traverses the nuclear volume, thus spreading its transverse momentum due to multiple scattering. Recently Bodwin and Lepage and I have explained the quantum mechanical origin of formation zone physics in terms of the destructive interference of inelastic amplitudes that occur on two different scattering centers in the nuclear target.[17] The discussion in that paper for the suppression of inelastic interactions of the incoming anti-quark in Drell-Yan massive lepton pair reactions can be carried over directly to the suppression of final state interactions of the struck quark in electroproduction.

5. Shadowing and Anti-Shadowing

One of the most striking nuclear effects seen in the deep inelastic structure functions is the depletion of the effective number of nucleons F_2^A/F_2^N in the region of low $x = x_{bj}$. The results from the EMC collaboration indicate that the effect is roughly Q^2-independent; *i.e.* shadowing is a leading twist in the operator product analysis. In contrast, the shadowing of the real photo-absorption cross section due to $\rho-$dominance falls away as an inverse power of Q^2.

Shadowing is a destructive interference effect which causes a diminished flux and interactions in the interior and back face of the nucleus. The Glauber analysis of hadron-nucleus scattering corresponds to the following: the incident hadron scatters elastically on a nucleon N_1 on the front face of the nucleus. At high energies the phase of the amplitude is imaginary. The hadron then propagates through the nucleus to nucleon N_2 where it interacts inelastically. The accumulated phase of the propagator is also i so that this multi-scattering amplitude is coherent and opposite in phase to the amplitude where the beam hadron interacts directly on N_2 without initial-state interactions. Thus the target nucleon N_2 sees less incoming flux; it is shadowed by elastic interactions on the front face of the nucleus. If the hadron-nucleon cross section is large, then the effective number of nucleons participating in the inelastic interactions is reduced to $\sim A^{2/3}$, the number of surface nucleons.

In the case of virtual photo-absorption, the photon converts to a $q\bar{q}$ pair at a distance proportional to $\omega = x^{-1} = 2p\cdot q/Q^2$ laboratory frame. The nuclear structure function F_2^A can then be written as an integral over the inelastic cross section $\sigma_{\bar{q}A}(s')$ where s' grows as $1/x$ for fixed space-like $\bar{q}$ mass. Thus the $A-$dependence of the cross section is equivalent to the shadowing of the $\bar{q}$ interactions in the nucleus. Recently Hung Lu and I have applied the standard Glauber multi-scattering theory, assuming that formalism can be taken over to off-shell $\bar{q}$ interactions.[18] Our results show that for reasonable values of the $\bar{q}$-nucleon cross section, one can easily understand the magnitude of the shadowing effect at small x. Moreover, if one introduces a $\alpha_R \simeq \frac{1}{2}$ Reggeon contribution to the $\bar{q}N$ amplitude, the real part of the phase introduced by such a contribution automatically leads to "anti-shadowing" at $x \sim 0.1$ (effective number of nucleons $F_2^A(x,Q)/F_2^N(x,Q) > A$) of the few percent magnitude seen by the SLAC and EMC experiments.

Our analysis provides the input or starting point for the $\log Q^2$ evolution of the deep inelastic structure functions. The parameters for the effective quark-nucleon cross section required to understand shadowing phenomena provide important information on the interactions of quarks and gluons in nuclear matter.

The above analysis also has implications for the nature of particle production for virtual photo-absorption in nuclei. At high Q^2 and $x > 0.3$, hadron production should be uniform throughout the nucleus. At low x or at low Q^2, where shadowing occurs the inelastic reaction occurs mainly at the front

surface. These features can be examined in detail by studying non-additive multiparticle correlations in both the target and current fragmentation regions.

6. Color Transparency

A striking feature of the QCD description of exclusive processes is color transparency: the only part of the hadronic wavefunction that scatters at large momentum transfer is its valence Fock state where the quarks are at small relative impact separation. Such a fluctuation has a small color-dipole moment and thus has negligible interactions with other hadrons. Since such a state stays small over a distance proportional to its energy, this implies that quasi-elastic hadron-nucleon scattering at large momentum transfer as illustrated in Fig. 3 can occur additively on all of the nucleons in a nucleus with minimal attenuation due to elastic or inelastic final state interactions in the nucleus, *i.e.* the nucleus becomes "transparent." By contrast, in conventional Glauber scattering, one predicts strong, nearly energy-independent initial and final state attenuation. A detailed discussion of the time and energy scales required for the validity of the PQCD prediction is given by Farrar *et al.* and Mueller in Ref. 5.

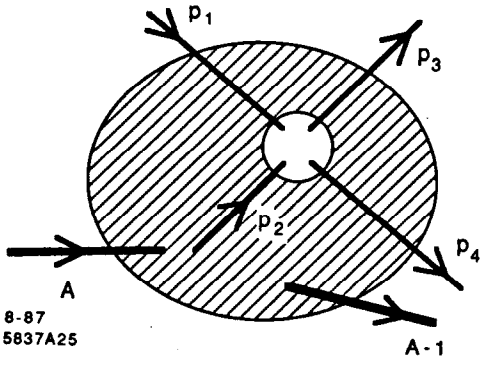

Figure 3. Quasi-elastic pp scattering inside a nuclear target. Normally one expects such processes to be attenuated by elastic and inelastic interactions of the incident proton and the final state interaction of the scattered proton. Perturbative QCD predicts minimal attenuation; *i.e.* "color transparency," at large momentum transfer.[5]

A recent experiment[19] at BNL measuring quasi-elastic $pp \to pp$ scattering at $\theta_{cm} = 90°$ in various nuclei appears to confirm the color transparency prediction—at least for p_{lab} up to 10 GeV/c (see Fig. 4). Descriptions of elastic scattering which involve soft hadronic wavefunctions cannot account for the data. However, at higher energies, $p_{lab} \sim$ 12 GeV/c, normal attenuation is observed in the

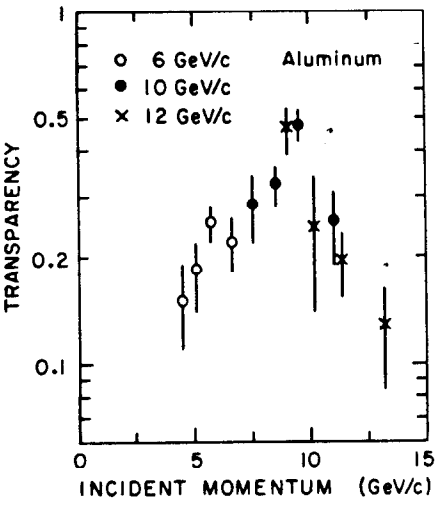

Figure 4. Measurements of the transparency ratio

$$T = \frac{Z_{eff}}{Z} = \frac{d\sigma}{dt}[pA \to p(A-1)]/\frac{d\sigma}{dt}[pA \to pp]$$

near 90° on Aluminum.[19] Conventional theory predicts that T should be small and roughly constant in energy. Perturbative QCD[5] predicts a monotonic rise to $T = 1$.

BNL experiment. This is the same kinematical region $E_{cm} \sim 5$ GeV where the large spin correlation in A_{NN} are observed.[20] Both features may be signaling new s-channel physics associated with the onset of charmed hadron production[21] or interference with Landshoff pinch singularity diagrams[22] Clearly, much more testing of the color transparency phenomena is required, particularly in quasi-elastic lepton-proton scattering, Compton scattering, antiproton-proton scattering, etc. The cleanest test of the PQCD prediction is to check for minimal attenuation in large momentum transfer lepton-proton scattering in nuclei since there are no complications from pinch singularities or resonance interference effects.

It should also be noted that initial-state interactions in the exclusive process $\bar{p}p \to \bar{\ell}\ell$ are suppressed at high lepton pair mass. This is a remarkable consequence of gauge theory and is quite contrary to normal treatments of initial interactions based on Glauber theory. This novel effect can be studied in quasielastic $\bar{p}A \to \bar{\ell}\ell\,(A-1)$ reaction. in which there are no extra hadrons produced and the produced leptons are coplanar with the beam. (The nucleus $(A-1)$ can be left excited). Since PQCD predicts the absence of initial-state elastic and inelastic interactions, the number of such events should be strictly

additive in the number Z of protons in the nucleus, every proton in the nucleus is equally available for short-distance annihilation. In traditional Glauber theory only the surface protons can participate because of the strong absorption of the $\bar{p}$ as it traverses the nucleus.

The above description is the ideal result for large s. QCD predicts that additivity is approached monotonically with increasing energy, corresponding to two effects: a) the effective transverse size of the $\bar{p}$ wavefunction is $b_\perp \sim 1/\sqrt{s}$, and b) the formation time for the $\bar{p}$ is sufficiently long, such that the Fock state stays small during transit of the nucleus.

7. Exclusive Channels in Electroproduction

One of the most important areas of exploration in coincident electroproduction experiments are exclusive channels. One can study not only the form factors of mesons and baryons at high Q^2 but also study electroproduction of resonances, testing not only dimensional scaling rules, but also consequences of gluon spin, such as the hadron helicity conservation rule. Exclusive channels are important since they are sensitive not only to the hard scattering quark-gluon diagrams, but also because of their sensitivity to the shape of the hadron distribution amplitude, the basic valence wavefunction of the hadron. It is also extremely interesting to extend measurements of the fixed angle behavior of photoproduction $d\sigma/dt(\gamma p \to \pi^+ n)$ to the virtual photon case. The perturbative QCD prediction is that the transverse photon amplitude is insensitive to Q^2 if $Q^2 << p_T^2$; this is dramatic consequences to vector meson dominance predictions which require that the rate falls off as Q^{-4}.

Electromagnetic Form Factors

We begin with a review of perturbative QCD predictions for form factors. A helicity conserving baryon form factor at large Q^2 has the form:[23] [see Fig. 5(a)]

$$F_B(Q^2) = \int_0^1 [dy] \int_0^1 [dx]\ \phi_B^\dagger(y_j, Q)$$
$$T_H(x_i, y_j, Q)\phi_B(x_i, Q)$$

where to leading order in $\alpha_s(Q^2)$, T_H is computed from $3q+\gamma^* \to 3q$ tree graph amplitudes: [Fig. 5(b).]

$$T_H = \left[\frac{\alpha_s(Q^2)}{Q^2}\right]^2 f(x_i, y_j)$$

and

$$\phi_B(x_i, Q) = \int [d^2k_\perp]\ \psi_V(x_i, \vec{k}_{\perp i})\theta(k_{\perp i}^2 < Q^2)$$

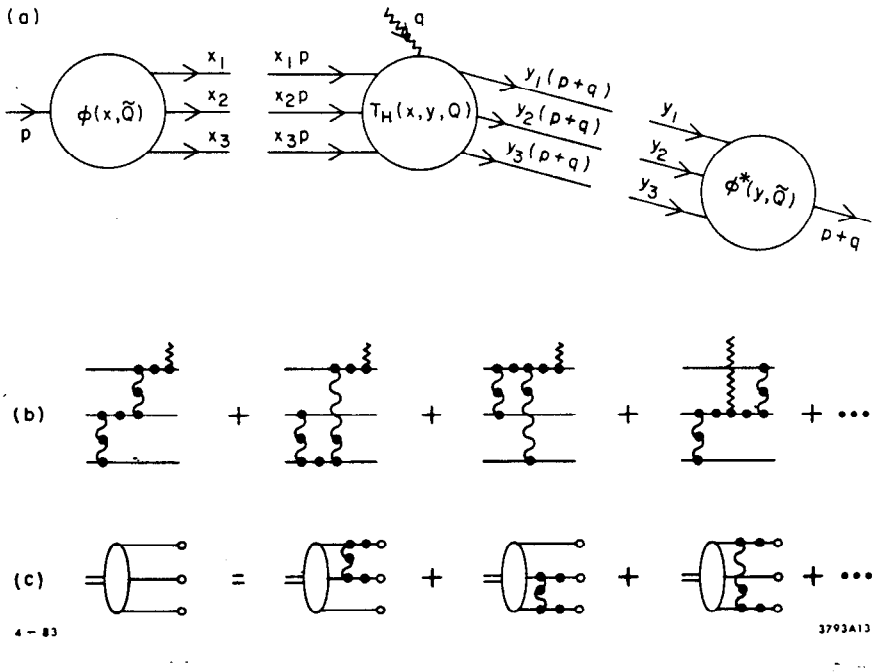

Figure 5. (a) Factorization of the nucleon form factor at large Q^2 in QCD. (b) The leading order diagrams for the hard scattering amplitude T_H. The dots indicate insertions which enter the renormalization of the coupling constant. (c) The leading order diagrams which determine the Q^2 dependence of the distribution amplitude $\phi(x, Q)$.

is the valence three-quark wavefunction [Fig. 5(c)] evaluated at quark impact separation $b_\perp \sim \mathcal{O}(Q^{-1})$. The net result for the nucleon magnetic form factor is

$$G_M(Q^2) = \left[\frac{\alpha_s(Q^2)}{Q^2}\right]^2 \sum_{n,m} a_{nm} \left(\log \frac{Q^2}{\Lambda^2}\right)^{-\gamma_n-\gamma_m} \times \left[1 + \mathcal{O}(\alpha_s(Q)) + \mathcal{O}\left(\frac{1}{Q}\right)\right].$$

The first factor, in agreement with the quark counting rule, is due to the hard scattering of the three valence quarks from the initial to final nucleon direction. Higher Fock states lead to form factor contributions of successively higher order in $1/Q^2$. The logarithmic corrections derive from an evolution equation for the nucleon distribution amplitude. The γ_n are the computed anomalous dimensions, reflecting the short distance scaling of three-quark composite operators.[24] The results hold for any baryon to baryon vector or axial vector transition amplitude that conserves the baryon helicity. Helicity non-conserving form factors should fall as an additional power of $1/Q^2$.[25] Measurements[26] of the transition form factor to the $J = 3/2$ $N(1520)$ nucleon resonance are consistent with $J_z = \pm 1/2$ dominance, as predicted by the helicity conservation rule.[25] It is important to explicitly verify that $F_2(Q^2)/F_1(Q^2)$ decreases at large Q^2. The angular distribution decay of the $J/\psi \to p\bar{p}$ is consistent with the QCD prediction $\lambda_p + \lambda_{\bar{p}} = 0$.

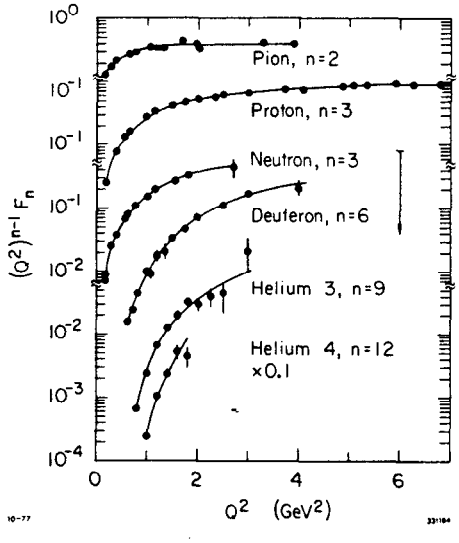

Figure 6. Comparison of experiment[27] with the QCD dimensional counting rule $(Q^2)^{n-1}F(Q^2) \sim$ *constant* for form factors. The proton data extends beyond 30 GeV^2.

Thus, modulo logarithmic factors, one obtains a dimensional counting rule for any hadronic or nuclear form factor at large Q^2 ($\lambda = \lambda' = 0$ or $1/2$)

$$F(Q^2) \sim \left(\frac{1}{Q^2}\right)^{n-1},$$

$$F_1^N \sim \frac{1}{Q^4}, \quad F_\pi \sim \frac{1}{Q^2}, \quad F_d \sim \frac{1}{Q^{10}},$$

where n is the minimum number of fields in the hadron. Since quark helicity is conserved in T_H and $\phi(x_i, Q)$ is the $L_z = 0$ projection of the wavefunction, total hadronic helicity is conserved at large momentum transfer for any QCD exclusive reaction. The dominant nucleon form factor thus corresponds to $F_1(Q^2)$ or $G_M(Q^2)$; the Pauli form factor $F_2(Q^2)$ is suppressed by an extra power of Q^2. Similarly, in the case of the deuteron, the dominant form factor has helicity $\lambda = \lambda' = 0$, corresponding to $\sqrt{A(Q^2)}$.

The comparison of experimental form factors with the predicted nominal power-law behavior is shown in Fig. 6. The general form of the logarithmic corrections to the leading power contributions form factors can be derived from the operator product expansion at short distance[24,28] or by solving an evolution equation[23] for the distribution amplitude computed from gluon exchange [Fig. 5(c)], the only QCD contribution which falls sufficiently slowly at large transverse momentum to effect the large Q^2 dependence.

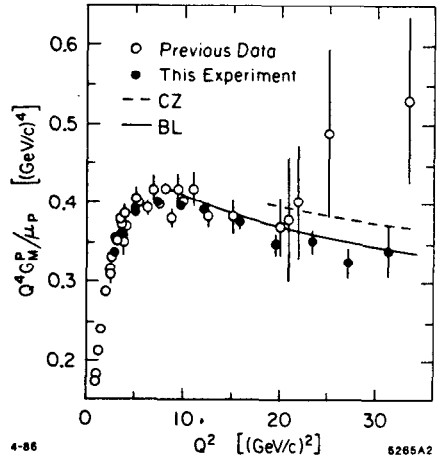

Figure 7. Comparison of the scaling behavior of the proton magnetic form factor with the theoretical predictions of Refs. 23 and 30. The CZ predictions[30] are normalized in sign and magnitude. The data are from Ref. 29.

The comparison of the proton form factor data with the QCD prediction arbitrarily normalized is

shown in Fig. 7. The fall-off of $(Q^2)^2 G_M(Q^2)$ with Q^2 is consistent with the logarithmic fall-off of the square of QCD running coupling constant. As we shall discuss below, the QCD sum rule[30] model form for the nucleon distribution amplitude together with the QCD factorization formulae, predicts the correct sign and magnitude as well as scaling behavior of the proton and neutron form factors.[29]

A crucial check of the perturbative QCD formalism is the verification of the color transparency phenomena, particularly for quasi-elastic electron-proton scattering in nuclei. As we have emphasized in Section 6, the observation of color transparency in the BNL experiment for quasi-elastic proton-proton scattering appears to have eliminated alternative models[31] in which exclusive scattering is dominated by soft hadron wavefunction contributions.

8. Hadronic Wavefunction Phenomenology

Let us now return to the question of the normalization of exclusive amplitudes in QCD. It should be emphasized that because of the uncertain magnitude of corrections of higher order in $\alpha_s(Q^2)$, comparisons with the normalization of experiment with model predictions could be misleading. Nevertheless, we shall assume that the leading order normalization is at least approximately accurate. If the higher order corrections are indeed small, then the normalization of the proton form factor at large Q^2 is a non-trivial test of the distribution amplitude shape; for example, if the proton wave function has a non-relativistic shape peaked at $x_i \sim 1/3$ then one obtains the wrong sign for the nucleon form factor. Furthermore symmetrical distribution amplitudes predict a very small magnitude for $Q^4 G_M^p(Q^2)$ at large Q^2.

The phenomenology of hadron wavefunctions in QCD is now just beginning. Constraints on the baryon and meson distribution amplitudes have been recently obtained using QCD sum rules and lattice gauge theory. The results are expressed in terms of gauge-invariant moments $< x_j^m > = \int \Pi dx_i \; x_j^m \; \phi(x_i, \mu)$ of the hadron's distribution amplitude. A particularly important challenge is the construction of the baryon distribution amplitude. In the case of the proton form factor, the constants a_{nm} in the QCD prediction for G_M must be computed from moments of the nucleon's distribution amplitude $\phi(x_i, Q)$. There are now extensive theoretical efforts to compute this nonperturbative input directly from QCD. The QCD sum rule analysis of Chernyak *et al.*[30,32] provides constraints on the first 12 moments of $\phi(x, Q)$. Using as a basis the polynomials which are eigenstates of the nucleon evolution equation, one gets a model representation of the nucleon distribution amplitude, as well as its evolution with the momentum transfer scale. The moments

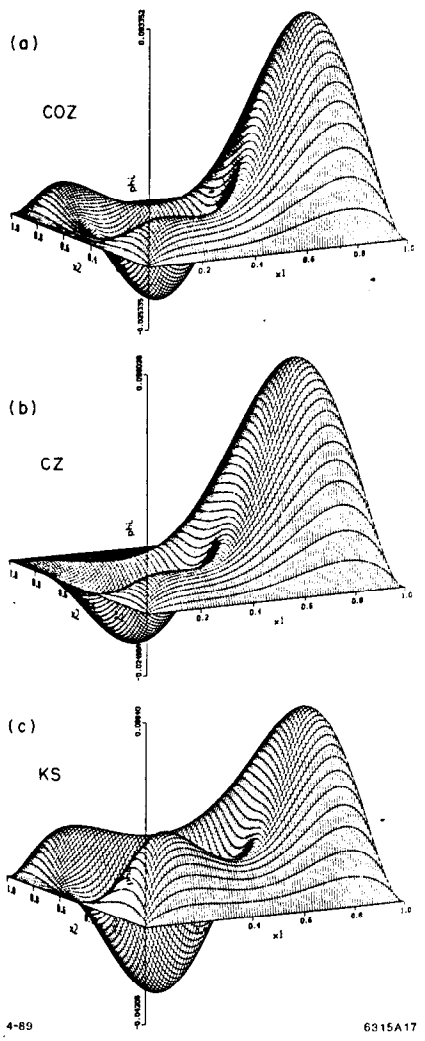

Figure 8. The proton distribution amplitude $\phi_p(x_i, \mu)$ determined at the scale $\mu \sim 1$ GeV from QCD sum rules.

of the proton distribution amplitude computed by Chernyak *et al.* have now been confirmed in an independent analysis by Sachrajda and King.[33]

A three-dimensional "snapshot" of the proton's *uud* wavefunction at equal light-cone time as deduced from QCD sum rules at $\mu \sim 1$ GeV by Chernyak *et al.*[32] and King and Sachrajda[33] is shown in Fig. 8. The QCD sum rule analysis predicts a surprising feature: strong flavor asymmetry in the nucleon's momentum distribution. The computed moments of the distribution amplitude imply that 65% of the proton's momentum in its 3-quark valence state is carried by the u-quark which has the same helicity as the parent hadron.

Dziembowski and Mankiewicz[34] have recently shown that the asymmetric form of the CZ distribution amplitude can result from a rotationally-invariant CM wave function transformed to the light cone using free quark dynamics. They find that one can simultaneously fit low energy phenomena (charge radii, magnetic moments, etc.), the measured high momentum transfer hadron form factors, and the CZ distribution amplitudes with a self-consistent ansatz for the quark wave functions. Thus for the first time one has a somewhat complete model for the relativistic three-quark structure of the hadrons. In the model the transverse size of the valence wave function is not found to be significantly smaller than the mean radius of the proton–averaged over all Fock states as argued in Ref. 35. Dziembowski *et al.* also find that the perturbative QCD contribution to the form factors in their model dominates over the soft contribution (obtained by convoluting the non-perturbative wave functions) at a scale $Q/N \approx 1$ GeV, where N is the number of valence constituents. (This criterion was also derived in Ref. 15.)

Gari and Stefanis[36] have developed a model for the nucleon form factors which incorporates the CZ distribution amplitude predictions at high Q^2 together with VMD constraints at low Q^2. Their analysis predicts sizeable values for the neutron electric form factor at intermediate values of Q^2.

A detailed phenomenological analysis of the nucleon form factors for different shapes of the distribution amplitudes has been given by Ji, Sill, and Lombard-Nelsen.[37] Their results show that the CZ wave function is consistent with the sign and magnitude of the proton form factor at large Q^2 as measured by the American University/SLAC collaboration[29] (see Fig. 9).

It should be stressed that the magnitude of the proton form factor is sensitive to the $x \sim 1$ dependence of the proton distribution amplitude, where non-perturbative effects could be important.[38] The asymmetry of the distribution amplitude emphasizes contributions from the large x region. Since non-leading corrections are expected when the quark propagator scale $Q^2(1-x)$ is small, in principle relatively large momentum transfer is required to clearly test the perturbative QCD predictions. Chernyak *et al.*[32] have studied this effect in some detail and claim that their QCD sum rule predictions are not significantly changed when higher moments of the distribution amplitude are included.

The moments of distribution amplitudes can also be computed using lattice gauge theory.[39] In the case of the pion distribution amplitudes, there is good agreement of the lattice gauge theory computations

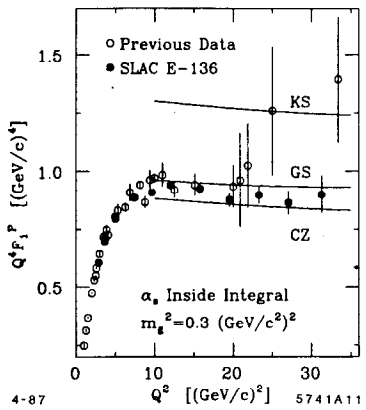

Figure 9. Predictions for the normalization and sign of the proton form factor at high Q^2 using perturbative QCD factorization and QCD sum rule predictions for the proton distribution amplitude (from Ref. 37). The predictions use forms given by Chernyak and Zhitnitsky, King and Sachrajda,[33] and Gari and Stefanis.[36]

of Martinelli and Sachrajda[40] with the QCD sum rule results. This check has strengthened confidence in the reliability of the QCD sum rule method, although the shape of the meson distribution amplitudes are unexpectedly structured: the pion distribution amplitude is broad and has a dip at $x = 1/2$. The QCD sum rule meson distributions, combined with the perturbative QCD factorization predictions, account well for the scaling, normalization of the pion form factor and $\gamma\gamma \to M^+M^-$ cross sections.

In the case of the baryon, the asymmetric three-quark distributions are consistent with the normalization of the baryon form factor at large Q^2 and also the branching ratio for $J/\psi \to p\bar{p}$. The data for large angle Compton scattering $\gamma p \to \gamma p$ are also well described.[41] However, a very recent lattice calculation of the lowest two moments by Martinelli and Sachrajda[40] does not show skewing of the average fraction of momentum of the valence quarks in the proton. This lattice result is in contradiction to the predictions of the QCD sum rules and does cast some doubt on the validity of the model of the proton distribution proposed by Chernyak *et al.*[32] The lattice calculation is performed in the quenched approximation with Wilson fermions and requires an extrapolation to the chiral limit.

The contribution of soft momentum exchange to the hadron form factors is a potentially serious complication when one uses the QCD sum rule model distribution amplitudes. In the analysis of Ref. 31 it was argued that only about 1% of the proton form factor comes from regions of integration in which all

the propagators are hard. A new analysis by Dziembowski *et al.*[42] shows that the QCD sum rule[30] distribution amplitudes of Chernyak *et al.*[30] together with the perturbative QCD prediction gives contributions to the form factors which agree with the measured normalization of the pion form factor at $Q^2 > 4\ GeV^2$ and proton form factor $Q^2 > 20\ GeV^2$ to within a factor of two. In the calculation the virtuality of the exchanged gluon is restricted to $|k^2| > 0.25\ GeV^2$. The authors assume $\alpha_s = 0.3$ and that the underlying wavefunctions fall off exponentially at the $x \simeq 1$ endpoints. Another model of the proton distribution amplitude with diquark clustering[43] chosen to satisfy the QCD sum rule moments comes even closer. Considering the uncertainty in the magnitude of the higher order corrections, one really cannot expect better agreement between the QCD predictions and experiment.

The relative importance of non-perturbative contributions to form factors is also an issue. Unfortunately, there is little that can be said until we have a deeper understanding of the end-point behavior of hadronic wavefunctions, and of the role played by Sudakov form factors in the end-point region. Models have been constructed in which non-perturbative effects persist to high Q.[31] However, such models do not seem consistent with the observation of color transparency. Other models have been constructed in which such effects vanish rapidly as Q increases.[44,45,34]

If the QCD sum rule results are correct then, the light hadrons are highly structured momentum-space valence wavefunctions. In the case of mesons, the results from both the lattice calculations and QCD sum rules show that the light quarks are highly relativistic. This gives further indication that while nonrelativistic potential models are useful for enumerating the spectrum of hadrons (because they express the relevant degrees of freedom), they may not be reliable in predicting wave function structure.

9. Diffractive Electroproduction

Exclusive processes such as virtual Compton scattering, $\gamma^* p \rightarrow \gamma p$, and ρ^0 electroproduction $\gamma^* p \rightarrow \rho^0 p$ play a special role in QCD as key probes of "pomeron" exchange and its possible basis in terms of multiple-gluon exchange. At large photon energy, the diffractive amplitudes are dominated by $J = 1$ Regge singularities.

Recent measurements of $\gamma^* p \rightarrow \rho^0 p$ by the EMC group[11] using the high energy muon beam at the SPS show three interesting features: (1) The ρ^0 is produced with zero helicity at $Q^2 \geq 1$ GeV^2; (2) the falloff in momentum transfer becomes remarkably flat for $Q^2 \geq 5$ GeV^2; and (3) the integrated cross section falls as $1/Q^4$.

The most surprising feature of the EMC data

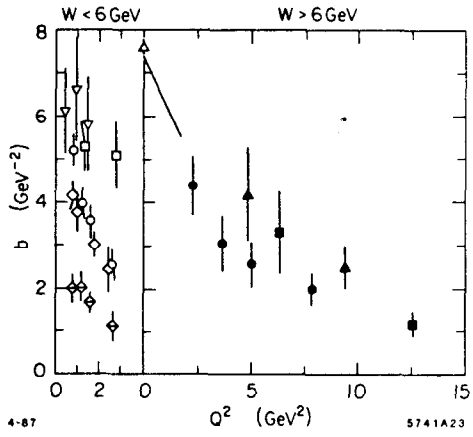

Figure 10. The slope parameter b for the form $d\sigma/dt = Ae^{bt'}$ fit to the EMC data (Ref. 11) for $\mu p \rightarrow \mu \rho^0 p$ for $|t'| \leq 1.5$ GeV^2.

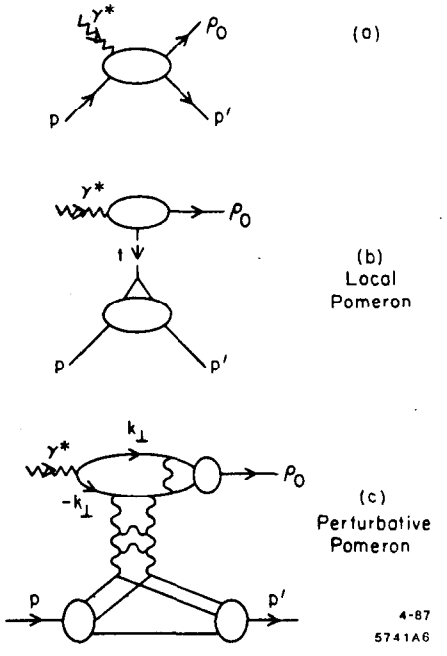

Figure 11. (a) Diffractive electroproduction of vector mesons. (b) Local pomeron contribution coupling to one quark. (c) Perturbative pomeron contribution. For large transverse momentum $k_t^2 \approx Q^2$ two-gluon exchange contributions are dominant.

is the very slow fall-off in t for the highest Q^2 data. (See Fig. 10.) Using the parameterization $e^{bt'}$, $t' = |t - t_{min}|$, the slope for $7 \leq Q^2 \leq 25$ GeV^2, $E_L = 200$ GeV data is $b \sim 2$ GeV^{-2}. If one assumes Pomeron factorization, then the fall-off in momentum transfer to the proton should be at least as fast as the square of the proton form factor,[46] representing the probability to keep the scattered proton intact. (See Fig. 11(b).) The predicted slope for $|t| < 1.5$ GeV^2 is $b \sim 3.4$ GeV^{-2}, much steeper than the EMC data. The background due to inelastic effects is estimated by the EMC group to be less than 20% in this kinematic domain.

In the vector meson dominance picture one expects: (1) dominantly transverse ρ polarization (s-channel helicity conservation); (2) fall-off in t similar to the square of the proton form factor (Pomeron factorization); and (3) a $1/Q^2$ asymptotic fall-off when longitudinal photons dominate.

The physics of electroproduction is quite different in QCD. At large $Q^2 \gg p_T^2$ diffractive channels take on a novel character. (See Fig. 11(c).) The transverse momentum k_T in the upper loop connecting the photon and ρ^0 is of order the photon mass scale, $k_T \sim Q$. (Other regions of phase space are suppressed by Sudakov form factors). Thus just as in deep inelastic inclusive scattering, the diffractive amplitude involves the proton matrix element of the product of operators near the light-cone. In the case of virtual Compton scattering $\gamma^* p \to \gamma p'$, one measures product of two electromagnetic currents. Thus one can test an operator product expansion similar to that which appears in deep inelastic lepton-nucleon scattering, but for non-forward matrix elements. In such a case the upper loop in Fig. 11(c) can be calculated using perturbative methods. The ρ enters through the same distribution amplitude that appears in large momentum transfer exclusive reactions. Since the gauge interactions conserve helicity, this implies $\lambda_\rho = 0$, $\lambda_p = \lambda'_p$ independent of the photon helicity. The predicted canonical Q^2 dependence is $1/Q^4$, which is also consistent with the EMC data.

Since the EMC data is at high energy ($E_\gamma = 200$ GeV, $s \gg p_T^2$) one expects that the vector gluon exchange diagrams dominate quark-exchange contributions. One can show that the virtuality of the gluons directly coupled to the $\gamma \to \rho$ transition is effectively of order Q^2, allowing a perturbative expansion. The effect is a known feature of the higher Born, multi-photon exchange contributions to massive Bethe Heitler processes in QED.[47]

The dominant exchange in the t-channel should thus be the two-gluon ladder shown in Fig. 11(c). This is analogous to the diagrams contributing to the evolution of the gluon structure function. If each gluon carries roughly half of the momentum transfer to different quarks in the nucleon, then the fall-off in t might be significantly slower than that of the proton form factor, since in the latter case the momentum transfer to the nucleon is due to the coupling to one quark. This result assumes that the natural fall-off of the nucleon wavefunction in transverse momentum is Gaussian rather than power-law at low momentum transfer. Alternatively the small slope of the differential cross section may reflect a sharp zero in the forward amplitude due to helicity mismatch between the photon and ρ.

In the case of quasi-elastic diffractive electroproduction in a nuclear target, we expect neither shadowing of the incident photon nor final state interactions of the outgoing vector meson at large Q^2 (color transparency).

Thus ρ^0 electroproduction and virtual Compton scattering can give important information on the nature of diffractive (pomeron exchange) processes. Data at all energies and kinematic regions are clearly essential.

10. Exclusive Nuclear Processes in QCD

An ultimate goal of QCD phenomenology is to describe the nuclear force and the structure of nuclei in terms of quark and gluon degrees of freedom. Explicit signals of QCD in nuclei have been elusive, in part because of the fact that an effective Lagrangian containing meson and nucleon degrees of freedom must be in some sense equivalent to QCD if one is limited to low-energy probes. On the other hand, an effective local field theory of nucleon and meson fields cannot correctly describe the observed off-shell falloff of form factors, vertex amplitudes, Z-graph diagrams, etc. because hadron compositeness is not taken into account. One of the most elegant areas of application of QCD to nuclear physics is the domain of large momentum transfer exclusive nuclear processes. Rigorous results have been given by Lepage, Ji and myself[48] for the asymptotic properties of the deuteron form factor at large momentum transfer. In the asymptotic $Q^2 \to \infty$ limit the deuteron distribution amplitude, which controls large momentum transfer deuteron reactions, becomes fully symmetric among the five possible color-singlet combinations of the six quarks. One can also study the evolution of the "hidden color" components (orthogonal to the np and $\Delta\Delta$ degrees of freedom) from intermediate to large momentum transfer scales; the results also give constraints on the nature of the nuclear force at short distances in QCD. The existence of hidden color degrees of freedom further illustrates the complexity of nuclear systems in QCD. It is conceivable that six-quark d^* resonances corresponds to these new degrees of freedom may be found by careful searches of the $\gamma^* d \to \gamma d$ and $\gamma^* d \to \pi d$ channels.

The basic scaling law for the helicity-conserving deuteron form factor is $F_d(Q^2) \sim 1/Q^{10}$ which comes from simple quark counting rules, as well as perturbative QCD. One cannot expect this asymptotic prediction to become accurate until very large Q^2 is reached since the momentum transfer has to be shared by at least six constituents. However there is a simple way to isolate the QCD physics due to the compositeness of the nucleus, not the nucleons. The deuteron form factor is the probability amplitude for the deuteron to scatter from p to $p+q$ but remain intact. Note that for vanishing nuclear binding energy $\epsilon_d \to 0$, the deuteron can be regarded as two nucleons sharing the deuteron four-momentum (see Fig. 12). The momentum ℓ is limited by the binding and can thus be neglected. To first approximation the proton and neutron share the deuteron's momentum equally. Since the deuteron form factor contains the probability amplitudes for the proton and neutron to scatter from $p/2$ to $p/2+q/2$; it is natural to define the reduced deuteron form factor[15,49,50]

$$f_d(Q^2) \equiv \frac{F_d(Q^2)}{F_{1N}\left(\frac{Q^2}{4}\right) F_{1N}\left(\frac{Q^2}{4}\right)}.$$

The effect of nucleon compositeness is removed from the reduced form factor. QCD then predicts the scaling

$$f_d(Q^2) \sim \frac{1}{Q^2}$$

i.e. the same scaling law as a meson form factor. Diagrammatically, the extra power of $1/Q^2$ comes from the propagator of the struck quark line, the one propagator not contained in the nucleon form factors. Because of hadron helicity conservation, the prediction is for the leading helicity-conserving deuteron form factor ($\lambda = \lambda' = 0$.) As shown in Fig. 13, this scaling is consistent with experiment for $Q = p_T \gtrsim 1$ GeV

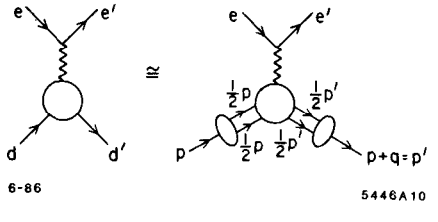

Figure 12. Application of the reduced amplitude formalism to the deuteron form factor at large momentum transfer.

The distinction between the QCD and other treatments of nuclear amplitudes is particularly clear in the reaction $\gamma d \to np$; *i.e.* photo-disintegration of the deuteron at fixed center of mass angle. Using dimensional counting, the leading power-law prediction from QCD is simply $\frac{d\sigma}{dt}(\gamma d \to np) \sim \frac{1}{s^{11}} F(\theta_{\rm cm})$.

Again we note that the virtual momenta are partitioned among many quarks and gluons, so that finite mass corrections will be significant at low to medium energies. Nevertheless, one can test the basic QCD dynamics in these reactions taking into account much of the finite-mass, higher-twist corrections by using the "reduced amplitude" formalism.[15,49,50] Thus the photo-disintegration amplitude contains the probability amplitude (*i.e.* nucleon form factors) for the proton and neutron to each remain intact after absorbing momentum transfers $p_p - 1/2p_d$ and $p_n - 1/2p_d$, respectively (see Fig. 14). After the form factors are removed, the remaining "reduced" amplitude should scale as $F(\theta_{\rm cm})/p_T$. The single inverse power of transverse momentum p_T is the slowest conceivable in any theory, but it is the unique power predicted by PQCD.

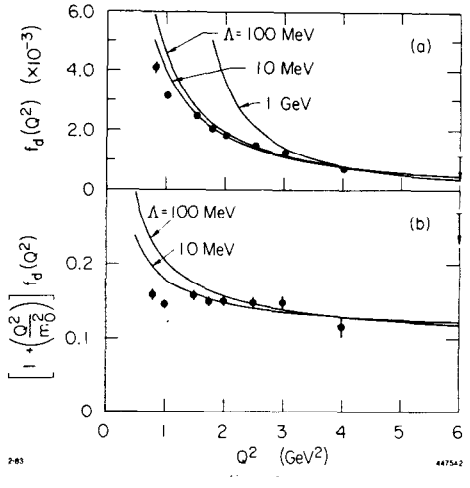

Figure 13. Scaling of the deuteron reduced form factor. The data are summarized in Ref. 15.

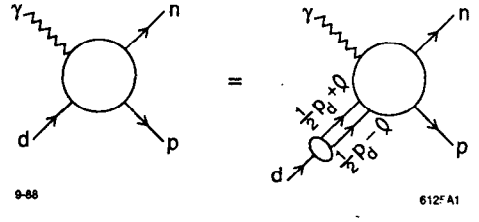

Figure 14. Construction of the reduced nuclear amplitude for two-body inelastic deuteron reactions.

The prediction that $f(\theta_{\rm cm})$ is energy dependent at high-momentum transfer is compared with experiment in Fig. 15. It is particularly striking to see the

QCD prediction verified at incident photon lab energies as low as 1 GeV. A comparison with a standard nuclear physics model with exchange currents is also shown for comparison as the solid curve in Fig. 15(a). The fact that this prediction falls less fast than the data suggests that meson and nucleon compositeness are not taken to into account correctly. An extension of these data to other angles and higher energy would clearly be very valuable.

An important question is whether the normalization of the $\gamma d \to pn$ amplitude is correctly predicted by perturbative QCD. A recent analysis by Fujita[54] shows that mass corrections to the leading QCD prediction are not significant in the region in which the data show scaling. However Fujita also finds that in a model based on simple one-gluon plus quark-interchange mechanism, normalized to the nucleon-nucleon scattering amplitude, gives a photo-disintegration amplitude with a normalization an order of magnitude below the data. However this model only allows for diagrams in which the photon insertion acts only on the quark lines which couple to the exchanged gluon. It is expected that including other diagrams in which the photon couples to the current of the other four quarks will increase the photo-disintegration amplitude by a large factor.

The derivation of the evolution equation for the deuteron and other multi-quark states is given in Refs. 55 and 50. In the case of the deuteron, the evolution equation couples five different color singlet states composed of the six quarks. The leading anomalous dimension for the deuteron distribution amplitude and the helicity-conserving deuteron form factor at asymptotic Q^2 is given in Ref. 55.

There are a number of related tests of QCD and reduced amplitudes which require $\bar{p}$ beams[50] such as $\bar{p}d \to \gamma n$ and $\bar{p}d \to \pi^- p$ in the fixed $\theta_{\rm cm}$ region. These reactions are particularly interesting tests of QCD in nuclei. Dimensional counting rules predict the asymptotic behavior $\frac{d\sigma}{dt}\,(\bar{p}d \to \pi^- p) \sim \frac{1}{(p_T^2)^{12}}\, f(\theta_{\rm cm})$ since there are 14 initial and final quanta involved. Again one notes that the $\bar{p}d \to \pi^- p$ amplitude contains a factor representing the probability amplitude (*i.e.* form factor) for the proton to remain intact after absorbing momentum transfer squared $\hat{t} = (p - 1/2p_d)^2$ and the $\overline{N}N$ time-like form factor at $\hat{s} = (\bar{p} + 1/2p_d)^2$. Thus $\mathcal{M}_{\bar{p}d \to \pi^- p} \sim F_{1N}(\hat{t})\, F_{1N}(\hat{s})\, \mathcal{M}_{\rm r}$, where $\mathcal{M}_{\rm r}$ has the same QCD scaling properties as quark meson scattering. One thus predicts

$$\frac{\frac{d\sigma}{d\Omega}\,(\bar{p}d \to \pi^- p)}{F_{1N}^2(\hat{t})\, F_{1N}^2(\hat{s})} \sim \frac{f(\Omega)}{p_T^2}\,.$$

The reduced amplitude scaling holds for $\gamma d \to pn$ at large angles and $p_T \gtrsim 1$ GeV (see Fig. 15). One thus expects similar precocious scaling behavior to hold for $\bar{p}d \to \pi^- p$ and other $\bar{p}d$ exclusive reduced amplitudes. Recent analyses by Kondratyuk and Sapozhnikov[56] show that standard nuclear physics wavefunctions and interactions cannot explain the magnitude of the data for two-body anti-proton annihilation reactions such as $\bar{p}d \to \pi^- p$.

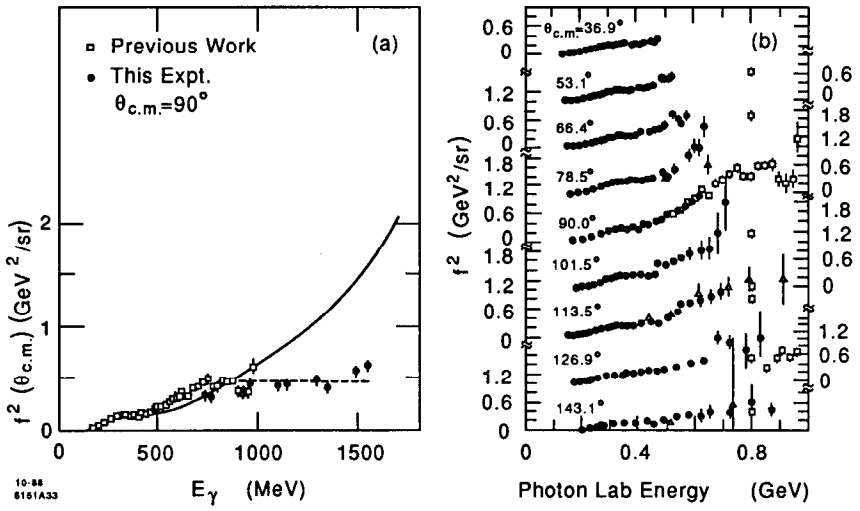

Figure 15. Comparison of deuteron photodisintegration data with the scaling prediction which requires $f^2(\theta_{cm})$ to be at most logarithmically dependent on energy at large momentum transfer. The data in (a) are from the recent experiment of Ref. 51. The nuclear physics prediction shown in (a) is from Ref. 52. The data in (b) are from Ref. 53.

11. Relation of Electroproduction to QCD Wavefunctions

As discussed in Section 8, constraints on moments of the hadron wavefunctions have been obtained using the "QCD Sum-Rule" technique and lattice gauge theory. An alternative non-perturbative method, "discretized light-cone quantization"[57] has recently been used to determine the hadronic and nuclear spectrum of QCD in one space and one time dimension in addition to the hadronic wavefunctions.

The simplest covariant representation of the hadron wavefunction in terms of its quark and gluon quanta is the light-cone Fock representation. One first constructs the complete set $|n><n| = \mathrm{I}$ of multi-quark and gluon color singlet eigenstates of the free QCD Hamiltonian at fixed light-cone time $\tau = t + z/c$. It is convenient to choose the physical light-cone gauge $A^+ = A^0 + A^z = 0$ since no ghosts are required. The expansion of the proton wavefunction on this basis at fixed τ has the form

$$\begin{aligned} |p> = \; & \psi_{uud}(x_i, k_{\perp i}, \lambda_i)|uud> \\ & + \psi_{uudg}(x_i, k_{\perp i}, \lambda_i)|uudg> \\ & + \psi_{uud\bar{q}\bar{q}}(x_i, k_{\perp i}, \lambda_i)|uud\bar{q}\bar{q}> \\ & + \ldots \end{aligned}$$

Each multiparticle wavefunction is a function of the light-cone fractions $x_i = (k_i^0 + k_i^z)/(P^0 + P^z)$, $\sum_1^n x_i = 1$ and transverse momenta $\sum_1^n k_{\perp i} = 0$. The rapidity of the constituent relative to that of the hadron is $y_i = \log x_i$. Since the x_i and $k_{\perp i}$ are defined as relative coordinates with respect to the hadron total momentum, the light-cone Fock state wavefunctions are frame-independent covariant amplitudes. In the non-relativistic limit the light-cone Fock expansion reduces to the momentum space representation of multiparticle n-body Schrödinger theory. The use of a Fock-state expansion in terms of free quark and gluons does not contradiction color confinement; the analog is the Fourier transform of the wavefunction of a particle bound in a harmonic oscillator.

Physical observables relevant to electroproduction can be immediately and simply related to the Fock-state wavefunctions. For example, form factors and other matrix elements of the electromagnetic current are given by a simple overlap of light-cone wavefunctions. Note that in the Bethe-Salpeter formalism, there is no closed expression for current matrix elements because of the presence of an infinite set of irreducible kernels. The structure functions for deep inelastic scattering are given by the usual parton-model expressions. Note that the sum is over all Fock components. The distribution amplitude which controls high momentum transfer exclusive reactions to leading only depends on the valence Fock state. Typical exclusive processes are given by the factorized form $M(s,t) = \int [dx]\ \Pi_I\ \phi_I(x, p_\perp)\ T_H(x_i, p_\perp, \theta_{cm})$. The hard scattering amplitude T_H is computed to leading order in $\alpha_s(p_\perp)$ by replacing each hadron by its valence quarks with momenta $p_i^\mu = x_i P^\mu$ collinear to its respective hadron. The main results are dimesional counting rules for the scaling behavior in $1/Q$ or $1/p_\perp$; hadron helicity conservation to leading order in $1/Q$ and color transparency.

Since high energy experiments have for the most part confirmed the main features of the quark and gluon scattering processes as predicted by perturbative QCD, the central problem in testing and understanding the full non-perturbative theory is the determination of the hadron wavefunctions themselves. Phenomenological constraints are obtained by comparing the predicted normalizations and angular behavior of exclusive cross sections with data particularly electroproduction. The main question is whether one can hope to evaluate the $\{\psi_n\}$ directly from theory. In principle, the most direct method would be to diagonalize the light-cone Hamiltonian for QCD in the Fock state basis: the eigenvalue problem is

$$H_{LC}^{QCD}|\Psi> = \mathcal{M}^2|\Psi>;$$

i.e. in Heisenberg matrix form

$$<n|H_{LC}^{QCD}|m><m|\Psi> = \mathcal{M}^2 <n|\Psi>;$$

To do this numerically one can introduce a discrete Fock basis by choosing periodic (anti-periodic for fermions) boundary conditions. The system is truncated in the ultraviolet by restricting the total invariant mass of the Fock basis. Thus far this program has been successfully carried for gauge theories such as QED and QCD($N_{color} = 2, 3, 4$) in one-space and one-time dimension.

Recently Hornbostel[58] has used discretized light-cone quantization (DLCQ) to obtain the complete color-singlet spectrum of QCD in one space and one time dimension for $N_C = 2, 3, 4$.

The hadronic spectra are obtained as a function of quark mass and QCD coupling constant (see Figs. 16 and 17). Where they are available, the spectra agree with results obtained earlier.

The structure functions for the lowest meson and baryon states in SU(3) at two different coupling strengths $m/g = 1.6$ and $m/g = 0.1$ are shown in Figs. 18 and 19. Higher Fock states have a very small probability; representative contributions to the baryon structure functions are shown in Figs. 20 and 21. For comparison, the valence wavefunction of a higher mass state which can be identified as a composite of meson pairs (analogous to a nucleus) is shown in Fig. 22. The interactions of the quarks in the pair state produce Fermi motion beyond $x = 0.5$.

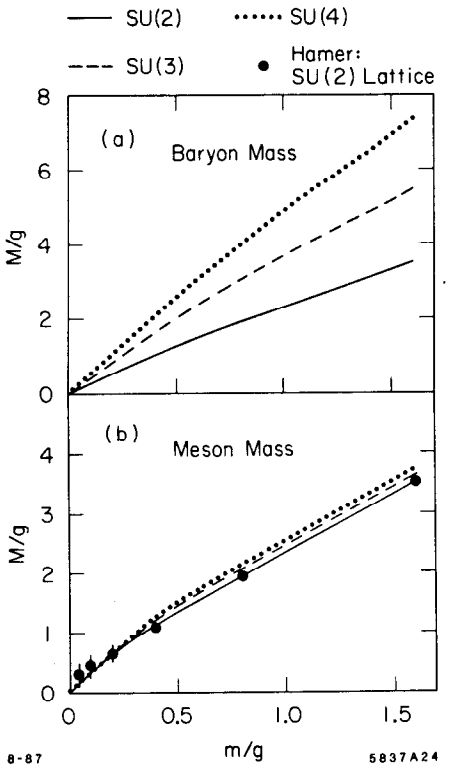

Figure 16. The baryon and meson spectrum in QCD [1+1] computed in DLCQ for $N_C = 2, 3, 4$ as a function of quark mass and coupling constant.[58]

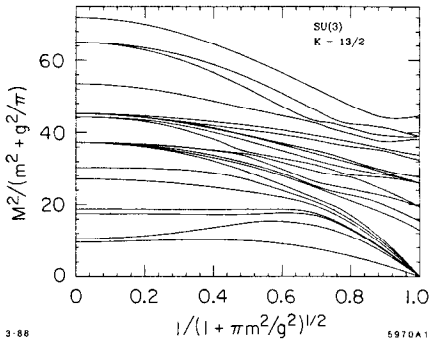

Figure 17. Representative baryon spectrum for QCD in one-space and one-time dimension.[58]

Although these results are for one time one space theory they do suggest that the sea quark distributions in physical hadrons may not be the smooth distributions usually assumed but actually they may be highly structured.

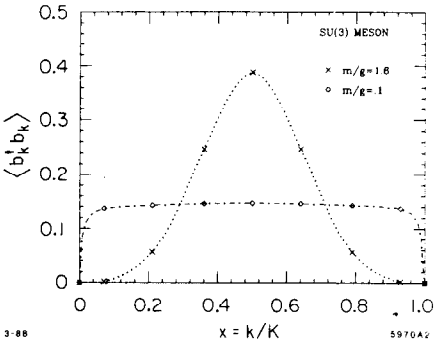

Figure 18. The meson quark momentum distribution in QCD[1+1] computed using DLCQ.[58]

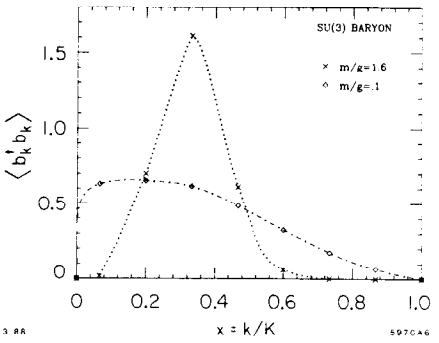

Figure 19. The baryon quark momentum distribution in QCD[1+1] computed using DLCQ.[58]

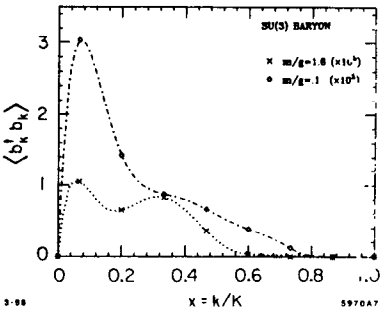

Figure 20. Contribution to the baryon quark momentum distribution from $qqq\overline{qq}$ states for QCD[1+1].[58]

12. Conclusions

Electroproduction is an extraordinarily rich phenomena; it remains the definitive process to examine the fundamental structure of the nucleon and nucleus since at momentum transfer beyond $Q^2 > 1\ GeV/c^2$

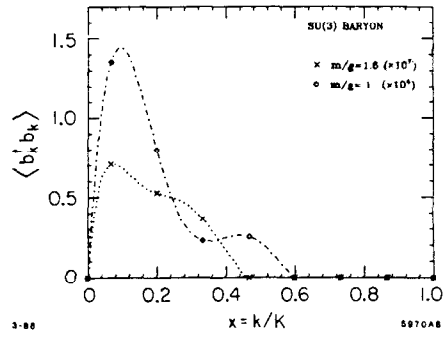

Figure 21. Contribution to the baryon quark momentum distribution from $qqq\bar{q}\bar{q}\bar{q}$ states for QCD[1+1].[58]

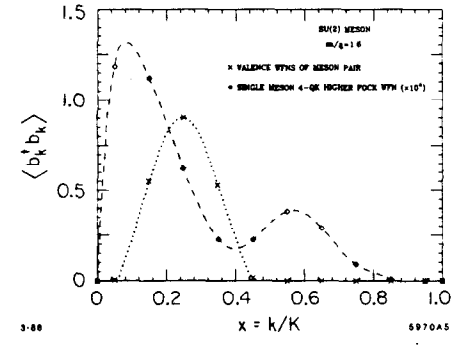

Figure 22. Comparison of the meson quark distributions in the $q\bar{q}q\bar{q}$ Fock state with that of a continuum meson pair state. The structure in the former may be due to the fact that these four-particle wavefunctions are orthogonal.[58]

the electron probes the quark current of hadronic and nuclear matter directly. Exclusive reactions and inclusive electroproduction measurements are complimentary coherent and incoherent probes of hadron structure and the underlying quark and gluon dynamical mechanisms. Measurements of the target spin correlations with final state hadron spins are also very important for unraveling the source of the apparently large net gluon and strange quark polarization in the nucleon. Photon reactions, both real and virtual, test other fundamental aspects as the quark current, including charge-cubed sum rules and isolation of the real part of the Compton amplitude. The nucleus in electroproduction serves both as a QCD structure and a perturbing environment to filter and select new aspects of hadron dynamics and quark hadronization. The structure of the proton and nuclear effects in QCD has become a common goal of both nuclear and particle physics. Internal targets in electron storage rings appears to be an ideal way to carry out virtually all of the above measurements.

REFERENCES

1. A. V. Crewe, Science 154, 729 (1966).
2. S. Bethke, LBL-26958, (1989).
3. S. J. Brodsky, G. P. Lepage, P. B. Mackenzie, Phys. Rev. D28, 228 (1983.)
4. See *e.g.* S. J. Brodsky, J. Ellis and M. Karliner, Phys. Lett. 206B, 309 (1988).
5. A. H. Mueller, Proc. XVII Recontre de Moriond (1982); S. J. Brodsky, Proc. XIII Int. Symp. on Multiparticle Dynamics, Volendam (1982). See also G. Bertsch, A. S. Goldhaber, and J. F. Gunion, Phys. Rev. Lett. 47, 297 (1981); G. R. Farrar, H. Liu, L. L. Frankfurt, M. J. Strikmann, Phys. Rev. Lett. 61, 686 (1988); A. H. Mueller, CU-TP-415, talk given at the DPF meeting, Stoors, Conn (1988), and CU-TP-412 talk given at the Workshop on Nuclear and Particle Physics on the Light-Cone, Los Alamos, (1988); B. Pire and J. P. Ralston, these proceedings.
6. Further discussion will appear in S. J. Brodsky and I. Schmidt, to be published. For a corresponding example in atomic physics see M. L. Goldberger and F. E. Low, Phys. Rev. 176, 1778 (1968).
7. J.F. Gunion, P. Nason and R. Blankenbecler, Phys. Rev. D29, 2491 (1984); Phys. Lett. 117B, 353 (1982).
8. J.F. Gunion, S.J. Brodsky and R. Blankenbecler, Phys. Rev. D8, 287 (1973); Phys. Lett. 39B, 649 (1972); D. Sivers, S.J. Brodsky and R. Blankenbecler, Phys. Reports 23C, 1 (1976). Extensive references to fixed angle scattering are given in this review.
9. E.L. Berger and S.J. Brodsky, Phys. Rev. D24, 2428 (1981).
10. E.L. Berger and F. Coester, ANL-HEP-PR-87-13 (1987).
11. J.J. Aubert *et al.*, Phys. Lett. 123B, 275 (1983); For a recent review see E.L. Berger and F. Coester, ANL-HEP-PR-87-13 (to be published in Ann. Rev. of Nucl. Part. Sci.).
12. P. Hoodbhoy and R.L. Jaffe, Phys. Rev. D35, 113 (1987); R.L. Jaffe, CTP #1315 (1985).
13. I.A. Schmidt and R. Blankenbecler, Phys. Rev. D15, 3321 (1977).
14. S.J. Brodsky and G.R. Farrar, Phys. Rev. Lett. 31, 1153 (1973); Phys. Rev. D11, 1309 (1975).
15. S.J. Brodsky and B.T. Chertok, Phys. Rev. Lett. 37, 269 (1976); Phys. Rev. D114, 3003 (1976).

16. S.J. Brodsky and G.P. Lepage, Phys. Rev. D24, 1808 (1981). The next to leading order evaluation of T_H for these processes is given by B. Nezic, Ph.D. Thesis, Cornell Univ. (1985).

17. G. T. Bodwin, S. J. Brodsky, and G. P. Lepage, Phys. Rev. D39, 3287 (1989).

18. S. J. Brodsky and Hung Lu, in preparation.

19. A. S. Carroll, *et al.*, Phys. Rev. Lett. 61, 1698 (1988).

20. G. R. Court *et al.*, Phys. Rev. Lett. 57, 507 (1986).

21. S. J. Brodsky and G. de Teramond, Phys. Rev. Lett. 60, 1924 (1988).

22. J. P. Ralston and B. Pire, Phys. Rev. Lett. 57, 2330 (1986); Phys. Lett. 117B, 233 (1982).

23. G. P. Lepage and S. J. Brodsky, Phys. Rev. D22, 2157 (1980); Phys. Lett. 87B, 359 (1979); Phys. Rev. Lett. 43, 545, 1625(E) (1979).

24. M. Peskin, Phys. Lett. 88B, 128 (1979); A. Duncan and A. H. Mueller, Phys. Lett. 90B, 159 (1980); Phys. Rev. D 21, 1636 (1980).

25. S. J. Brodsky and G. P. Lepage, Phys. Rev. D24, 2848 (1981).

26. V. D. Burkert, CEBAF-PR-87-006.

27. M. D. Mestayer, SLAC-Report 214 (1978) F. Martin, *et al.*, Phys. Rev. Lett. 38, 1320 (1977); W. P. Schultz, *et al.*, Phys. Rev. Lett. 38, 259 (1977); R. G. Arnold, *et al.*, Phys. Rev. Lett. 40, 1429 (1978); SLAC-PUB-2373 (1979); B. T. Chertok, Phys. Lett. 41, 1155 (1978); D. Day, *et al.*, Phys. Rev. Lett. 43, 1143 (1979). Summaries of the data for nucleon and nuclear form factors at large Q^2 are given in B. T. Chertok, in Progress in Particle and Nuclear Physics, Proceeding of the International School of Nuclear Physics, 5th Course, Erice (1978), and Proceedings of the XVI Rencontre de Moriond, Les Arcs, Savoie, France, 1981.

28. S.J. Brodsky, Y. Frishman, G.P. Lepage and C. Sachrajda, Phys. Lett. 91B, 239 (1980).

29. R. G. Arnold *et al.*, Phys. Rev. Lett. 57, 174 (1986).

30. V. L. Chernyak and I. R. Zhitnitskii, Phys. Rept. 112, 1783 (1984). Xiao-Duang Xiang, Wang Xin-Nian and Huang Tao, BIHEP-TH-84, 23 and 29, 1984.

31. N. Isgur and C.H. Llewellyn Smith, Phys. Rev. Lett. 52, 1080 (1984). G. P. Korchemskii, A. V. Radyushkin, Sov. J. Nucl. Phys. 45, 910 (1987) and references therein.

32. V. L. Chernyak, A. A. Ogloblin and I. R. Zhitnitsky, Novosibirsk preprints INP 87-135,136, and references therein. See also Xiao-Duang Xiang, Wang Xin-Nian, and Huang Tao, BIHEP-TH-84, 23 and 29, 1984, and M. J. Lavelle, ICTP-84-85-12; Nucl. Phys. B260, 323 (1985).

33. I. D. King and C. T. Sachrajda, Nucl. Phys. B279, 785 (1987).

34. Z. Dziembowski and L. Mankiewicz, Phys. Rev. Lett. 58, 2175 (1987); Z. Dziembowski, Phys. Rev. D37, 768, 778, 2030 (1988)

35. G. P. Lepage, S. J. Brodsky, Tao Huang and P. B. Mackenzie, published in the *Proceedings of the Banff Summer Institute*, 1981.

36. M. Gari and N. Stefanis, Phys. Lett. B175, 462 (1986), M. Gari and N. Stefanis, Phys. Lett. 187B, 401 (1987).

37. C-R Ji, A. F. Sill and R. M. Lombard-Nelsen, Phys. Rev. D36, 165 (1987).

38. See also G. R. Farrar, presented to the Workshop on Quantum Chromodynamics at Santa Barbara, 1988.

39. S. Gottlieb and A. S. Kronfeld, Phys. Rev. D33, 227-233 (1986); CLNS-85/646, June 1985.

40. G. Martinelli and C. T. Sachrajda, Phys. Lett. 190B, 151, 196B, 184, (1987); Phys. Lett. B217, 319, (1989).

41. G. W. Atkinson, J. Sucher, and K. Tsokos, Phys. Lett. 137B, 407 (1984); G. R. Farrar, E. Maina, and F. Neri, Nucl. Phys. B259, 702 (1985) Err.-ibid. B263, 746 (1986).; E. Maina, Rutgers Ph.D. Thesis (1985); J. F. Gunion, D. Millers, and K. Sparks, Phys. Rev. D33, 689 (1986); P. H. Damgaard, Nucl. Phys. B211, 435 (1983); B. Nezic, Ph.D. Thesis, Cornell University (1985); D. Millers and J. F. Gunion, Phys. Rev. D34, 2657 (1986).

42. Z. Dziembowski, G. R. Farrar, H. Zhang, and L. Mankiewicz, contribution to the 12th Int. Conf. on Few Body Problems in Physics, Vancouver, 1989.

43. Z. Dziembowski and J. Franklin contribution to the 12th Int. Conf. on Few Body Problems in Physics, Vancouver, 1989.

44. C. Carlson and F. Gross, Phys. Rev. Lett. 53, 127 (1984); Phys. Rev. D36 2060 (1987).

45. O. C. Jacob and L. S. Kisslinger, Phys. Rev. Lett. 56, 225 (1986).

46. A. Donnachie and P.V. Landshoff, Phys. Lett. 185B, 403 (1987).

47. S.J. Brodsky, J.F. Gunion and D. Soper, SLAC-PUB-4193 (1987).

48. S.J. Brodsky, C.-R. Ji and G.P. Lepage, Phys. Rev. Lett. 51, 83 (1983).

49. S.J. Brodsky and J.R. Hiller, Phys. Rev. C28, 475 (1983).

50. C. R. Ji and S. J. Brodsky, Phys. Rev. D34, 1460 (1986); D33, 1951, 1406, 2653, (1986). For a review of multi-quark evolution, see S. J. Brodsky, C.-R. Ji, SLAC-PUB-3747, (1985).

51. J. Napolitano *et al.*, ANL preprint PHY–5265–ME–88 (1988).

52. T. S.-H. Lee, ANL preprint (1988).

53. H. Myers *et al.*, Phys. Rev. 121, 630 (1961); R. Ching and C. Schaerf, Phys. Rev. 141, 1320 (1966); P. Dougan *et al.*, Z. Phys. A 276, 55 (1976).

54. T. Fujita, MPI-Heidelberg preprint, 1989.

55. S. J. Brodsky, C.-R. Ji, G. P. Lepage, Phys. Rev. Lett. 51, 83 (1983).

56. L.A. Kondratyuk and M. G. Sapozhnikov, Dubna preprint E4-88-808.

57. T. Eller, H. C. Pauli and S. J. Brodsky, Phys. Rev. D35, 1493 (1987).

58. K. Hornbostel, SLAC-0333, Dec 1988; K. Hornbostel, S. J. Brodsky, and H. C. Pauli, SLAC-PUB-4678, Talk presented to Workshop on Relativistic Many Body Physics, Columbus, Ohio, June, 1988.